

LA-UR- 98-833

Approved for public release;  
distribution is unlimited.

Title:

TIME-GATED ENERGY-SELECTED COLD NEUTRON  
RADIOGRAPHY

CONF-980337--

Author(s):

Thomas E. McDonald (P-23), Torben O. Brun (LANSCE-12), Thomas N. Claytor (ESA-MT), Eugene H. Farnum (MST-5), Geoffrey L. Greene (LANSCE-DO), and Christopher Morris (P-25)

Submitted to:

Third International Topical Meeting on  
Neutron Radiography New Detectors,  
Imaging Techniques and Applications,  
3/6/98, Lucerne, Switzerland  
for publication in Nuclear Instruments  
and Methods in Physics Research, Section  
A

DISTRIBUTION OF THIS DOCUMENT IS UNLIMITED 

MASTER

**Los Alamos**  
NATIONAL LABORATORY

Los Alamos National Laboratory, an affirmative action/equal opportunity employer, is operated by the University of California for the U.S. Department of Energy under contract W-7405-ENG-36. By acceptance of this article, the publisher recognizes that the U.S. Government retains a nonexclusive, royalty-free license to publish or reproduce the published form of this contribution, or to allow others to do so, for U.S. Government purposes. Los Alamos National Laboratory requests that the publisher identify this article as work performed under the auspices of the U.S. Department of Energy. The Los Alamos National Laboratory strongly supports academic freedom and a researcher's right to publish; as an institution, however, the Laboratory does not endorse the viewpoint of a publication or guarantee its technical correctness.

## **DISCLAIMER**

This report was prepared as an account of work sponsored by an agency of the United States Government. Neither the United States Government nor any agency thereof, nor any of their employees, makes any warranty, express or implied, or assumes any legal liability or responsibility for the accuracy, completeness, or usefulness of any information, apparatus, product, or process disclosed, or represents that its use would not infringe privately owned rights. Reference herein to any specific commercial product, process, or service by trade name, trademark, manufacturer, or otherwise does not necessarily constitute or imply its endorsement, recommendation, or favoring by the United States Government or any agency thereof. The views and opinions of authors expressed herein do not necessarily state or reflect those of the United States Government or any agency thereof.

## **DISCLAIMER**

**Portions of this document may be illegible  
in electronic image products. Images are  
produced from the best available original  
document.**

## Time-Gated Energy-Selected Cold Neutron Radiography

Thomas E. McDonald, Jr., Torben O. Brun, Thomas N. Claytor  
Eugene H. Farnum, Geoffrey L. Greene, and Christopher Morris

Los Alamos National Laboratory, Los Alamos, NM, 87545, USA

### ABSTRACT

A technique is under development at the Los Alamos Neutron Science Center (LANSCE), Manuel Lujan Jr. Neutron Scattering Center (Lujan Center) for producing neutron radiography using only a narrow energy range of cold neutrons. The technique, referred to as Time-Gated Energy-Selected (TGES) neutron radiography, employs the pulsed neutron source at the Lujan Center with time of flight to obtain a neutron pulse having an energy distribution that is a function of the arrival time at the imager. The radiograph is formed on a short persistence scintillator and a gated, intensified, cooled CCD camera is employed to record the images, which are produced at the specific neutron energy range determined by the camera gate. The technique has been used to achieve a degree of material discrimination in radiographic images. For some materials, such as beryllium and carbon, at energies above the Bragg cutoff the neutron scattering cross section is relatively high while at energies below the Bragg cutoff the scattering cross section drops significantly. This difference in scattering characteristics can be recorded in the TGES radiography and, because the Bragg cutoff occurs at different energy levels for various materials, the approach can be used to differentiate among these materials. This paper outlines the TGES radiography technique and shows an example of radiography using the approach.

**Keywords:** cold neutron radiography, energy specific radiography, time-gated energy-selected radiography, materials discrimination

## BACKGROUND

Cold neutron radiography (CNR) at specific energies or a narrow range of energies in the few meV is being developed at the Los Alamos Neutron Science Center (LANSCE), Manuel Lujan Jr. Neutron Scattering Center (Lujan Center), Los Alamos National Laboratory, as a technique in non-destructive testing and evaluation. Neutron radiography is attractive because of the strong variation of neutron scattering cross sections as a function of energy that is exhibited by materials. As a result of this strong variation, measurement of the intensity as a function of neutron energy and sample position can be used to give elemental and spatial information of an object. In addition, by using neutron energies in the millielectron volt (meV) regime, it is possible to exploit an important behavior of the scattering cross sections in crystalline materials. For a number of materials, below an energy of a few meV (the exact energy depends on the material) there is an abrupt drop in the scattering cross section when the wavelength reaches twice the largest lattice spacing of the material [1]. Table I shows the Bragg cut-off of some selected materials. By carrying out neutron radiography at specific neutron energies it is possible to distinguish materials of differing crystal structures. For example, a radiograph taken at an energy above the Bragg cut-off of all materials comprising a device would show the entire device assuming the materials have sufficiently high scattering cross sections. However, choosing an energy below the Bragg cutoff of some materials and above the Bragg cutoff of others produces a radiograph in which those materials having a Bragg cutoff above the energy where the radiograph is made will exhibit much less scattering and will show up lighter in the radiograph. Thus, it is possible by judiciously choosing the neutron energy at which a radiograph is made to separate components and materials in a sample or device. These component images can likely be separated through signal processing. In addition, imaging in three dimensions can be obtained using tomographic image reconstruction techniques.

Radiography at specific energies (or narrow range of energies) is possible at LANSCE by exploiting the short, intense neutron pulse produced in the spallation source combined with time-of-flight techniques. Such radiography is generally not exploited in a reactor environment because the steady state nature of the neutron source is not favorable to separating neutrons of differing energies. In addition, this technique has the advantage over thermal and resonance neutron radiography by emphasizing the abrupt cross-section change rather than relying on the slower variation of cross section with thermal neutron energies or the presence of a useful neutron resonance cross section.

### **TIME-GATED ENERGY-SELECTED RADIOGRAPHY CONCEPT**

The basic concept for carrying out neutron radiography using only a narrow range of neutron energies, which we refer to as Time-Gated Energy-Selected (TGES) neutron radiography, is illustrated in Figure 1. A short neutron pulse is formed at the beginning of the flight path at time  $t_0$ . The pulse travels to the end of the flight path where it is spread temporally with the more energetic (faster) neutrons arriving ahead of the lower energy (slower) neutrons. The arrival time of neutrons at the end of the flight path is proportional to the inverse of the square root of the neutron energy. The object to be radiographed and imager are positioned at the end of the flight path to record the radiographic data. The image is formed on a scintillator that has a short persistence compared to the shutter time of the imager. The gate (shutter) width,  $t_g$ , of the imager is adjusted to record the radiographic data over a range of neutron energies by adjusting the gate opening to occur at the time of arrival at the sample of the highest energy neutrons to be used in making the radiograph and adjusting the closing time to occur at the time of arrival of the lowest energy neutrons. The time from  $t_0$  to the gate opening, which is the travel time along the flight path of the highest energy neutrons making the radiograph, is referred to as the gate delay time,  $\Delta T$ . Thus, the gate delay,  $\Delta T$ , essentially determines the energy at which the radiograph is made and the gate width,  $t_g$ , determines the energy resolution at which the

radiograph is made. This technique, for which a patent disclosure has been submitted, was first demonstrated at the LANSCE, Lujan Center.

## NEUTRON BEAM CHARACTERISTICS

The neutron spallation source at the Lujan Center of LANSCE [2] provides neutron pulses at a frequency of 20 pulses/s. The neutron pulse is produced by the interaction of an 800 MeV proton beam pulse from the LANSCE accelerator onto a tungsten target. The neutron pulse width at the tungsten target is approximately 270 ns. The target has a split configuration with a 14-cm gap between the upper component of the target, which has a 10-cm diameter and 7-cm length, and the lower component, which has a 10-cm diameter and 23-cm length. The neutron production facility is designed for up to 16 flight paths. The cold neutron radiography beam line is installed on flight path 11a. The neutron pulse on flight path 11a is moderated by a water moderator and a liquid hydrogen moderator to shift the energy spectrum toward the low energy region. A shutter for beam line 11 is installed in the biological shield surrounding the target. A 12-m beam guide consisting of 8, 1.5-m sections transports the beam from the exit port of the shutter to a shielded experiment room, referred to as a cave. The shutter and guides were purchased from and installation supervised by the French Company, Cilas. The guides have a <sup>58</sup>Ni coating and a square aperture 6 cm on a side. Figure 2 is a photograph showing the 6-cm square exit opening of the beam guide with an aluminum vacuum window over the end. The total length of the flight path from the tungsten target to the end of the beam guide is approximately 19.5 m. An engineering drawing showing the 8 sections of guides and guide stands is given in Figure 3. At a length of 19.5 m, the flight time of 5-meV neutrons is approximately 8 ms and an imaging gate width of 100 microseconds provides an energy resolution of 0.065 meV. These timing and gating parameters are easily achieved with presently available imaging equipment.

Flight path 11a is positioned such that the axis of the beam passes between the upper and lower target components (between the gap) of the split tungsten spallation target. Thus, gamma rays emanating directly from the spallation target are not in the correct geometry to enter the flight path and, as a result, the gamma contamination in the neutron beam is low. Average gamma content in the beam has been measured to be approximately 3.2  $\mu\text{R/s}$ . The total neutron flux at the exit of the flight path beam guide has been measured to be approximately  $2.1 \times 10^6$  neutrons/cm<sup>2</sup>/s at a proton current of approximately 75  $\mu\text{A}$ .

Beam divergence is due primarily to the critical angle of the beam guides, which is energy dependent. At 1 meV the critical angle is approximately 1 degree. An L/D measurement that was made on the exit beam compares favorably with the 1-degree divergence at the 1-meV critical angle. Beam non-uniformity was measured to be less than 10%. A summary of beam characteristics is given in Table II.

### SCINTILLATOR SCREEN

The scintillator screen used in the TGES experiments is a commercially available product, BC704, which is available from Bicron, Newbury, Ohio, facility. The scintillator material is based on ZnS(Ag) and <sup>6</sup>Li [3]. The wavelength of maximum emission is in the blue at 450 nm. The light emission decay time is approximately 200 ns, which is more than adequate for the 100  $\mu\text{s}$  and longer gate time used in the experiments. The absolute scintillation efficiency is approximately 9%. Each thermal neutron stopped by the scintillator produces  $1.75 \times 10^5$  photons. Two configurations of the scintillator screen are available from the manufacturer, a standard screen mounted on a 1-mm thick aluminum plate and an unmounted, semi-rigid, stand-alone screen. The unmounted configuration was used in these experiments.

## GATED IMAGING SYSTEM

The gated imaging system used to record images formed on the scintillator consisted of an intensified, cooled CCD camera with a mirror placed at a 45 degree angle next to the scintillator to relay the image out of the beam path and a lens to focus the image onto the intensifier. The relay mirror is necessary because of the damage that would occur to the CCD sensor if placed in the neutron beam. The field of view of the imager can be set by adjusting the distances between the scintillator, lens, and camera. The intensifier is used to amplify the low light level from the scintillator and serves as a gate, or shutter, for the camera. A schematic diagram of the imaging system is shown in Figure 4.

The CCD in the camera has a 1024x1024 array of square pixels, 24 microns on a side. A 40-mm intensifier was used in the imager. A 200-mm f/2 lens was used to focus the image onto the intensifier and dimensions were set to achieve a field of view of approximately 2.1 cm, which, by calculation, is a resolution of approximately 21 line-pairs per mm. A resolution of approximately 20 line-pairs/mm of the lens, intensifier, and camera combination was measured using an Air Force resolution pattern, which is in close agreement with calculation. This system resolution allows features as small as approximately 100 microns to be visible in the image. The system was installed in a light tight enclosure to prevent stray light from being picked up by the intensifier and camera. Figure 5 is a photograph of the imaging system showing the turning mirror, camera, and camera controller. The scintillator is the white sheet mounted on the wall of the enclosure that is visible next to the mirror.

Control of the imager was accomplished in a straightforward manner with digital delay and pulse generators. An intensifier control unit supplied the intensifier gain voltage and gate pulse. Camera control was accomplished with a separate camera control unit (visible in

Figure 5 just under the camera), which monitored camera operation and performed frame readout and storage. A block diagram of the timing and control setup is shown in Figure 6. The intensifier control unit can provide gate widths ranging from 10  $\mu$ s to 1.8 ms, which was more than adequate for the TGES experiments.

### TGES RADIOGRAPHY RESULTS

A proof-of-principle demonstration of the TGES concept was carried out using two materials that have well defined Bragg cutoffs, beryllium, which has a Bragg cutoff at approximately 6 meV, and carbon, which has a cutoff at approximately 1.9 meV. A 25-mm thick beryllium block was obtained into which a one-half by 20 threaded hole was cut (one-half inch diameter and 20 threads per inch). A one-half by 20 carbon screw was inserted into the hole. Radiographs were made above, between, and below the Bragg cutoffs of the two materials. The results of the radiography is shown in Fig. 7. Fig. 7A is a radiograph taken at approximately 7.5 meV, which is above the Bragg cutoffs of the two materials. Above the Bragg cutoffs both the beryllium and carbon show up relatively dark in the radiograph because the scattering cross section in the two materials is high at this energy. The portion of the carbon bolt inside the beryllium cannot be observed. Fig. 7B is a radiograph taken at approximately 2.9 meV, which is between the Bragg cutoffs of the two materials, and the beryllium has become much lighter because the scattering cross section has significantly decreased while the carbon bolt remains relatively dark. That portion of the carbon inside the beryllium has now become visible. Fig. 7C is a radiograph taken at approximately 1.5 meV, which is below the Bragg cutoff of both materials. At this energy both materials have become light in the radiograph and that portion of the carbon in the beryllium is only faintly visible. Had the beryllium and carbon assembly obscured another item having a relatively high scattering cross section, it would now become evident.

## CONCLUSIONS

The feasibility of using the pulsed neutron spallation source at LANSCE to obtain radiographs of objects at specific or a narrow range of energies using time of flight and time gated imaging techniques has been demonstrated. We refer to the technique as time-gated energy-selected (TGES) neutron radiography. Material discrimination has been shown for two crystalline materials having large scattering cross section changes across the Bragg cutoff by obtaining radiographs above and below the Bragg cutoff energies of the materials and observing the differences in neutron transmission through the materials. Possible practical applications of this technique are currently under investigation. Simulations of TGES radiography is being carried out for various components and materials using a neutron transport code in order to identify those items that show potential for yielding good radiography results. Such potential applications include determining the percent saturation of desiccant and imaging components in encapsulated sub-assemblies. We plan to carry out TGES radiography on the most promising of these potential applications during the next run cycle of LANSCE.

## ACKNOWLEDGMENTS

The authors would like to acknowledge contributions to this effort by Robert Gallegos, Lloyd Hunt, Stephen Jaramillo, Russell Mortensen, Peter Pazuchanics, Joyce Roberts, Mark Schwalb, and Susan Seestrom.

## REFERENCES

1. Pynn, R. , Neutron Scattering A Primer, Los Alamos National Laboratory Report, LAUR-95-3840
2. See the LANSCE web site at [www.lansce.lanl.gov](http://www.lansce.lanl.gov)
3. A. R. Spowart, Optimizing Neutron Scintillators for Neutron Radiography, British Journal of Non-Destructive Testing, 11(1), 2-11, March 1969

## TABLES

**Table I**  
**Bragg Cut-off Energies of Some Selected Materials**

<u>Material</u>	<u>Energy (meV)</u>
Aluminum (Al)	4
Beryllium (Be)	6
Carbon (C)	2
Magnesium (Mg)	2.6 - 2.9
Silicon (Si)	2
Iron (Fe)	5
Nickel (Ni)	5
Lead (Pb)	3
Bismuth (Bi)	2
Zirconium (Zr)	2.5 - 3

**Table II**  
**Summary of FP11a Neutron Beam Characteristics**

Beam Size at Guide Aperture:	6 cm x 6 cm
Pulse Repetition Rate:	20 pulses/s
Flux Intensity:	$\sim 2.1 \times 10^6$ n/cm <sup>2</sup> /s
Gamma Ray Content:	$\sim 3.2 \mu\text{R/s}$
Non-uniformity:	< 10%
Beam Divergence:	1 mev: 1 degree

## FIGURE CAPTIONS

Figure 1. Diagram of Time-Gated Energy-Selected (TGES) neutron radiography concept. At time,  $t_0$ , a short, intense pulse of neutrons is emitted from the spallation source at the beginning of the flight path. When the pulse reaches the end of the flight path, it is expanded in energy and time. A radiograph using just a narrow range of energies is taken by gating the imager on for a gate width,  $t_g$ , when the neutron energies of interest arrive at the sample at time  $\Delta T$  after  $t_0$ . The gate delay time,  $\Delta T$ , determines the basic energy at which the radiograph is taken and the gate width,  $t_g$ , determines the narrow range of energies over which the radiograph is taken.

Figure 2. Photograph of beam guide taken in experiment room showing the 6-cm square exit aperture. An aluminum vacuum window is in place over the opening.

Figure 3. Engineering drawing of the CNR beam guide showing the 8, 1.5-m sections and stands.

Figure 4. Diagram of cold neutron radiography gated imager. The object to be radiographed is placed in the beam in front of the scintillator. The image is formed on the scintillator and relayed by mirror and lens to the intensified camera. The mirror is necessary due to the damage that would occur to the CCD if placed in the neutron beam. The lens defines the field of view and resolution of the image and the intensifier provides amplification of the low light levels from the scintillator and also serves as a gate (or shutter) for the camera.

Figure 5. Photograph of gated imager system showing light tight box, turning mirror, camera and camera controller. The scintillator is the white sheet mounted on the wall of the enclosure next to the turning mirror.

Figure 6. Block Diagram of Imaging System Control

Note: Figure 7 consists of three images, 7A, 7B, and 7C. The caption for each of the three images and the figure is given below.

Fig. 7A

Neutron Energy: 7.5 meV  
Above Cutoff of Be (6 meV)  
Above Cutoff of C (2 meV)  
Both Be; C Dark

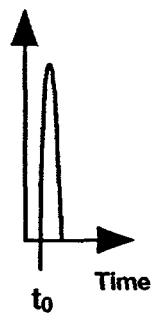
Fig. 7B

Neutron Energy: 2.9 meV  
Below Cutoff of Be  
Above Cutoff of C  
Be Light; C Dark

Fig. 7C

Neutron Energy: 1.5 meV  
Below Cutoff both Be and C  
Both Be and C Light

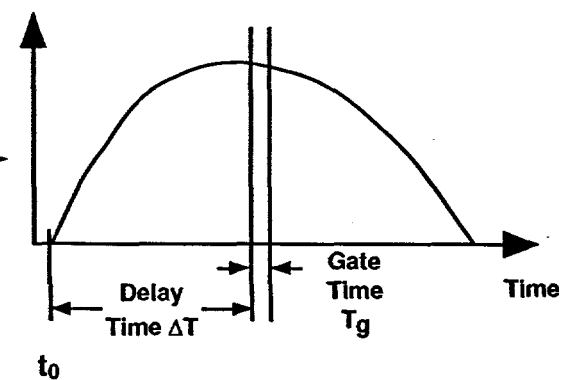
Fig. 7 Demonstration of cold neutron radiography using the TGES technique to obtain radiographs at specific neutron energies. These images demonstrate material discrimination using the Bragg cutoff phenomenon. The images are a series of radiographs of a carbon bolt threaded into a beryllium block. Image (A) is a radiograph taken at approximately 7.5 meV, which is above the Bragg cutoffs of both beryllium (6 meV) and carbon (2 meV) and shows both the beryllium and carbon relatively dark. Image (B) is a radiograph taken at approximately 2.9 meV, which is between the Bragg cutoffs of beryllium and carbon; the beryllium has become lighter due to the reduction in scattering cross-section across the Bragg cutoff and the carbon bolt inside the beryllium has become visible. Image (C) is a radiograph taken at a neutron energy of approximately 1.5 meV, which is below the Bragg cutoff of both beryllium and carbon and both the beryllium and carbon have become lightened. Note that if any denser material had been obscured by the beryllium and carbon it could be seen in Image C.



**Neutron Pulse**  
Beginning of Flight Path

Direction of Travel

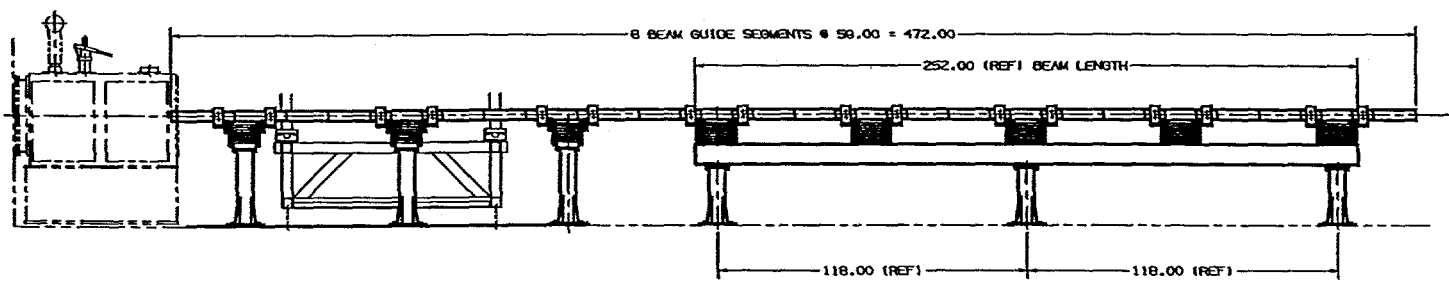
Flight Path

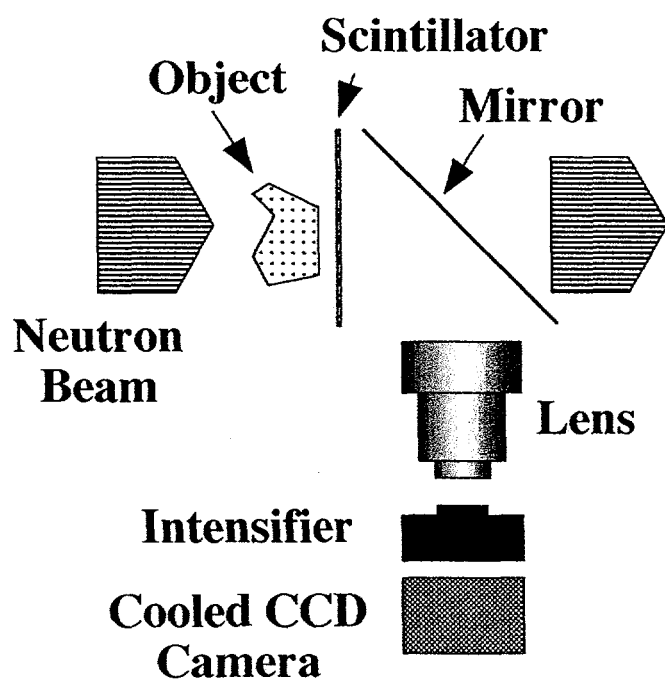


**Expanded Neutron Pulse**  
End of Flight Path



Fig 2





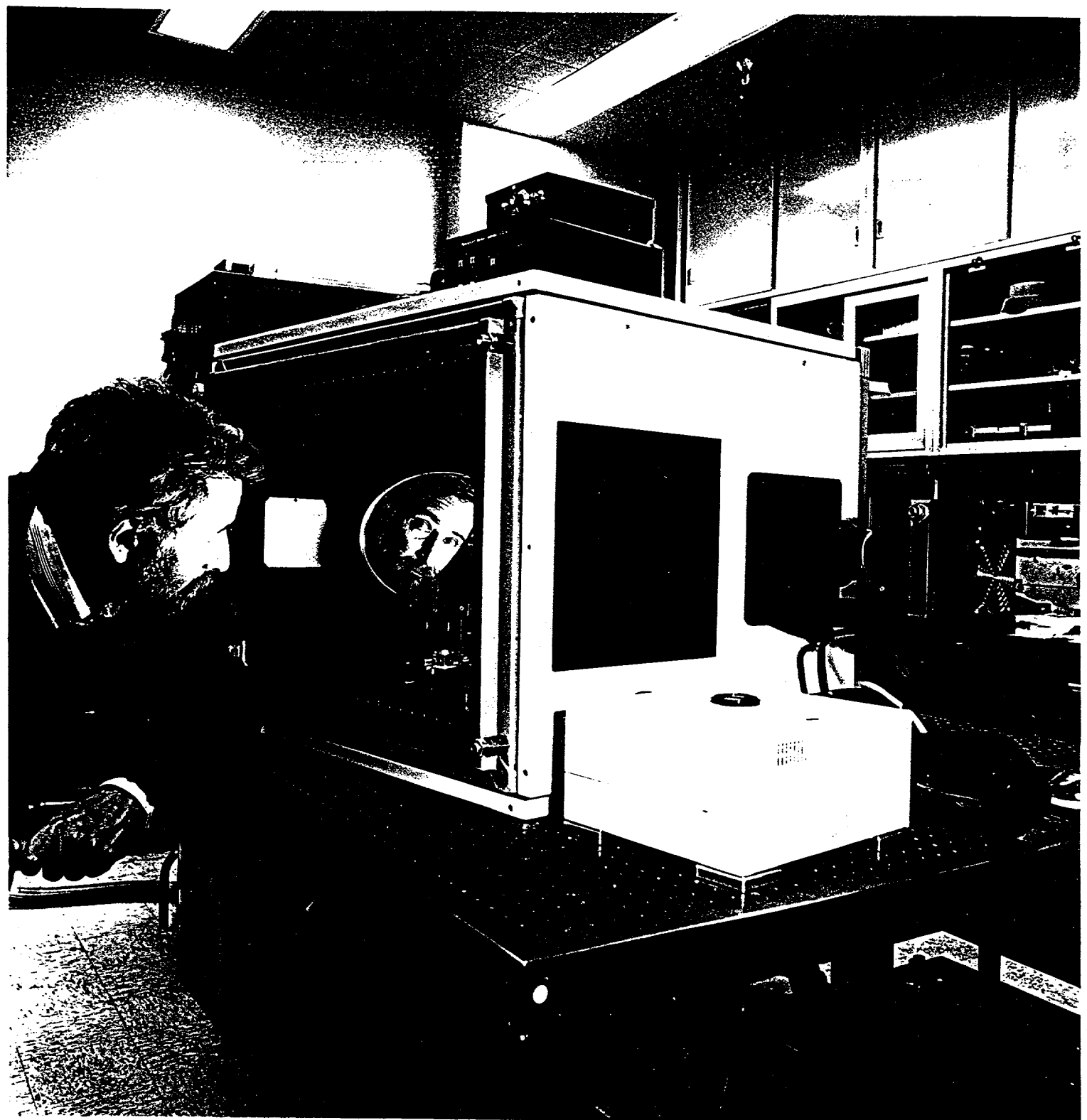
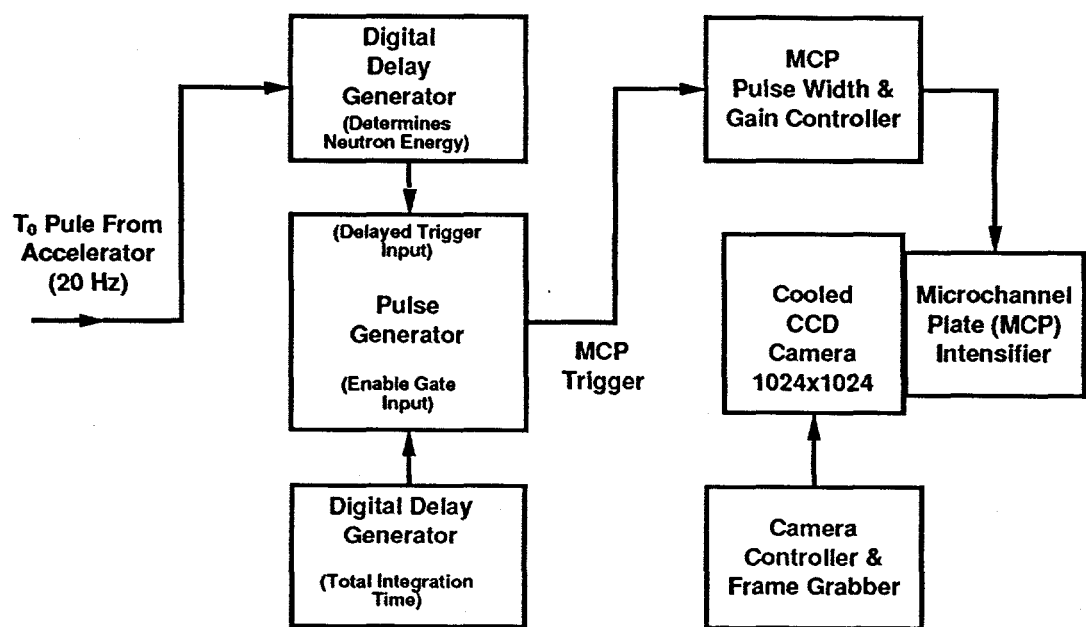


Fig 5



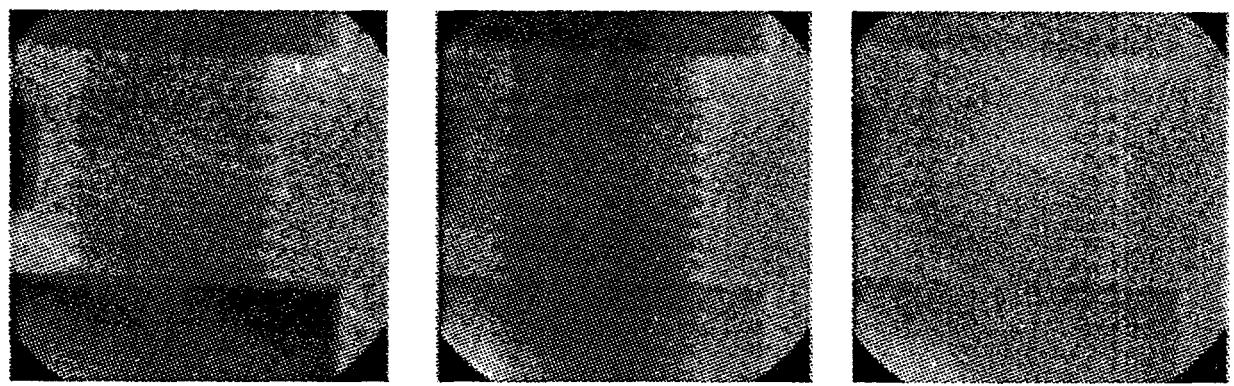


Fig 2